Canadian Conference - Pacific Conference on Earthquake Engineering 2023
Vancouver, British Columbia
June 25th – June 30th, 2023

Development and Hybrid Testing of Ring Spring Self-Centering Energy Dissipative Braces

Ahmed Hassan[1], Jeffrey Erochko[2*], Cameron Flude[3] and David Lau[4]

[1] Instructor of Structural Engineering, Department of Civil Engineering, Carleton University, Ottawa, ON, Canada
[2] Associate Professor of Structural Engineering, Department of Civil Engineering, Carleton University, Ottawa, ON, Canada
[3] PhD Student, Department of Civil Engineering, Carleton University, Ottawa, ON, Canada
[4] Professor of Structural Engineering, Department of Civil Engineering, Carleton University, Ottawa, ON, Canada
[*]jeffrey.erochko@carleton.ca (Corresponding Author)

ABSTRACT

Self-Centering systems aim to eliminate or minimize residual drifts in structures, leading to improved seismic performance and allowing immediate occupancy of structures post-earthquake. In this study a new compact Self-Centering Energy-Dissipative (SCED) brace is developed, designed, and experimentally tested. This new innovative, compact, high-capacity ring spring SCED (RS-SCED) brace exhibits a nonlinear response with good energy dissipation and post-yield stiffness, while preventing residual drift. The new RC-SCED brace utilizes ring springs to provide a restoring force, while simultaneously dissipating energy through friction between ring spring units in the assembly. The mechanism allows the brace to have a large deformation capacity without the need for a long tendon to provide a restoring force, resulting in a relatively short brace that can attain self-centering behaviour during the earthquake response of a building for drift demands up to 4% or more. The new RS-SCED brace has a high load capacity with stable and repeatable hysteresis that makes it suitable for full scale buildings in high seismic regions. Hybrid simulations are performed to evaluate the system level performance of the new brace in prototype structures. The hybrid simulation method allows for the realistic seismic assessment of critical structural components or subassemblies in a structure without the need to test the entire structure in a laboratory by combining experimental testing and numerical modelling together. In this study, an 8-storey building with the new ring spring SCED brace is tested using hybrid simulation. The physical test substructure is the prototype compact high-capacity ring spring SCED with a load capacity of 1400 kN and a deformation capacity of 160 mm. During the tests, the systems are subjected to a series of earthquake records with a wide range of frequency contents at different hazard levels. The brace maintained full force and deformation capacity and full self-centering behaviour throughout all the tests.

Keywords: Self-Centering Device, Hybrid Simulation.

INTRODUCTION

The 1994 Northridge earthquake in the United States and the 1995 Kobe earthquake in Japan caused significant damage to the infrastructure in urban areas with tragic loss of life and economic losses that exceeded $50 to $100 billion USD [1],[2]. From the lessons learned from these two events, the academic and structural engineering community shifted their focus towards developing performance-based earthquake engineering design methodologies. Using performance-based design, the anticipated structural performance during and after a major seismic event may be more predictable and reliable. Structures designed using performance-based methodology are required to meet performance criteria which are not limited to structural integrity, but also include criteria that correlate to safety of occupancy and functionality of the structure after an earthquake. Most performance-based design criteria are based on the maximum inter-storey drift experienced by a structure. In this investigation, the use of residual drift as an important performance criterion in addition to the maximum inter-storey drift is considered. The residual drift is defined as the permanent deformation that is sustained by the structure following a seismic event. The importance of residual drift to structural performance is demonstrated by a number of studies which focus on the effect of residual drift on building functionality, occupant comfort, rehabilitation cost and structural safety [3]-[7].

Other studies of non-structural systems through unidirectional wall system testing [8] and shake table tests [9] have found a strong correlation between significant damage to door systems and residual drift exceeding 0.5%, which seriously compromises safety and egress of occupants after an earthquake. A study by Erochko et al. [10] found that systems such as Buckling

Restrained Brace Frames (BRBFs) and Special Moment-resisting frame (SMRF) experience residual drifts in the range of 0.5-1.2% under design based earthquake hazards, but can reach as high as 2% to 4% under the hazard level of Maximum Credible Earthquake (MCE) and near fault earthquake events [10][11]. It was found that when the damaged structures were subjected to a second design level earthquake event, the structures would not exhibit the expected performance assumed under the design standard ASCE 7-05 [12] because of P-Delta effects that may compromise the building structural stability and safety [10].

Self-centering systems, such as rocking wall systems [13]-[18] and self-centering moment resisting frames [19]-[24], are viable options for protection of structures from excessive residual drifts after major seismic events. Self-centering systems rely on a structural mechanism that can accommodate significant drift without yielding, thus allowing the building to return to its original position after a seismic event. The main distinctive feature that separates self-centering systems from other Seismic Force Resisting Systems (SFRS) is the flag-shaped hysteresis. This flag shaped response results in the structure returning to its initial zero displacement position after each cycle of response, as shown in Figure 1 [25]. Due to this flag-shaped hysteresis, self-centering systems dissipate less energy than other typical high-performance SFRSs, which may exhibit a parallelogram shaped hysteresis. Since large-energy earthquakes tend to be characterized by only one or two maximum peaks in the excitation, the lack of energy dissipation is generally not a major disadvantage.

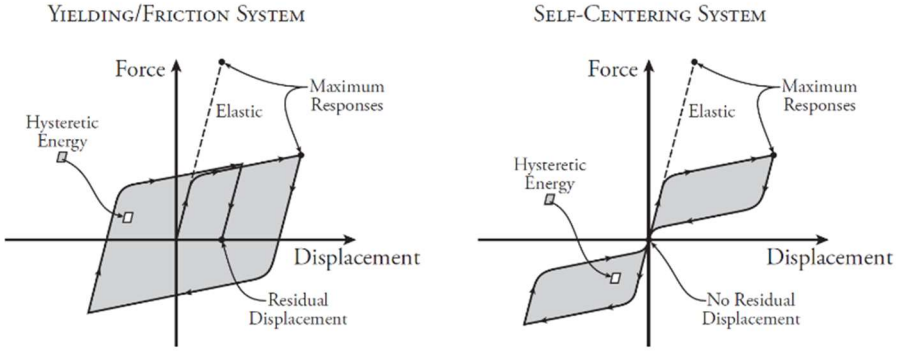

Figure 1: Non-linear Hysteresis response of Typical vs Self-Centering SFRS [25]

According to a survey of the existing building stock in Canada [26], 56% of the total floor space of commercial and institutional facilities was built prior to 1979 using old design standards with poor seismic detailing specifications. This, coupled with the observed poor seismic performance of buildings designed with CSA 1977 or earlier standards, clearly indicates that there is an urgent need to improve the performance of these existing deficient structures. Design with self-centering systems, such as rocking walls or self-centering MRFs, may be a viable option for improving the seismic performance of new construction, but these concepts are typically not appropriate for rehabilitation of existing structures. This has led the structural and research community to investigate alternative designs for self-centering braces which can be more easily applied in rehabilitation of existing structures.

Although many developments to self-centering braces have been suggested and evaluated in the past [27]-[34] , a need for compact self-centering braces with a large force and sufficient realistic deformation capacity still exists. The major challenge for the previously developed devices is their inability to have a large load capacity while also having a large deformation capacity. Even when these devices can provide sufficient load and deformation capacity, their required size and length is very large making them impractical to use in most structures. Ring springs have been utilized in a variety of self-centering systems but in many previous studies they were either inadequate for use in large structures due to their load and deformation capacity; or impractical for rehabilitation applications due to disturbance caused by construction [35]-[40]. Recent studies developed and tested new SCED braces with ring springs and used the test results in analytical models to show buildings with these braces integrated into their SFRS would have satisfactory seismic performance with minimal residual building drift. Wang et al. [41] developed a friction spring damper and tested a half-scale protypes that were able achieve a maximum axial force of up to 227.8 kN at a desired maximum deformation of 42.5mm and with no residual drift. Issa and Alam [42] developed a spring-based piston bracing system with a double friction spring configuration with a total length of 1.2 m. The brace reached a peak axial load of almost 60 kN during testing at a deformation of 40mm.

This paper presents the development and performance verification for a new innovative self-centering brace that has the double advantages of a high load and deformation capacity, while still maintaining a compact size compared to previously developed SCED braces. Previously developed SCED braces relied on aramid tendons with a peak strain of 1.8% resulting in the need for tendons in excess of 8 m in length to accommodate a high inter-storey drift demand of 4%. The proposed brace would accommodate the same level of drift demand with a spring that is only 1.2 m in length making it a feasible option for application in both new and existing structures. At this size, the brace can fit in most building bay sizes. The new Ring Spring Self-

Centering Energy Dissipative (RS-SCED) brace utilizes ring springs to achieve the self-centering capability and energy dissipation behaviour through friction without the need for external friction fuses.

DESIGN OF RS-SCED BRACE

Most SCED braces are limited in application by either their force or deformation capacity. SCED braces with a large load and deformation capacity require large size and length which presents challenges for implementing them in design of actual structures in engineering practice. These issues limit the practical utilization of SCED braces in large structures such as high-rise buildings. The design objectives for the new RS-SCED (Ring Spring Self-Centering Energy Dissipative) brace are to: 1) achieve a large deformation capacity equivalent to at least 4% drift in a 4-meter-high bay, 2) achieve a load capacity that is in excess of 1000 kN to be on a comparable order of magnitude to other lateral load resisting systems of large structures, 3) have a compact design which makes it easier to install the braces in both new construction and rehabilitation applications for existing structures, and 4) that can be fabricated using steel, a commonly used material in construction with well-established properties and behaviour familiar by the engineering profession, using readily available section sizes. The new design utilizes ring springs to provide both a large deformation and load capacities within a compact size. To evaluate the response characteristics of this brace both on its own and as the lateral load resisting system in different structural systems, a full-scale prototype of the brace was designed, built and tested.

Design of the New Ring Spring SCED Braces

The design of the prototype brace is chosen to validate the applicability and functionality of a brace with enough capacity to support multi-storey buildings. The list of design parameters for the prototype ring spring brace are shown in Table 1. The SCED brace ultimate load P_u is the maximum load capacity of the ring springs used in the assembly. This corresponds to the capacity of the largest commercially available ring spring that can fit in a commonly available steel shape, Ring Spring type 34000 provided by RingFeder [43]. The target activation load of the SCED brace P_a is determined through the design of a prototype 8-storey office building with a 4 m typical floor height, designed for seismic design category D according to the ASCE 7-16 [44] and using the first floor storey shear demand. The storey drift demand Δ_f of 4% is chosen to compare the response of this brace to other BRBs and SCED braces. This value is much larger than typical code drift limits and it represents a likely maximum drift when considering earthquake variability. The deformation capacity of each brace δ_b is calculated based on the intended floor drift demand Δ_f and the height of the relevant floor h. The number of ring elements in the assembly can be calculated based on the deformation capacity of the brace δ_b and the deformation capacity of a single element S_e.

Table 1: Ring Spring SCED Design Parameters

Parameter	Value
SCED brace ultimate load ($\boldsymbol{P_u}$)	1450 kN
SCED brace activation load ($\boldsymbol{P_a}$)	406 kN
SCED brace pre-compression ($\boldsymbol{PC}$)	28%
Storey Drift ($\boldsymbol{\Delta_f}$)	4% (132 mm)
Element Spring travel ($\boldsymbol{S_e}$)	7.5mm
Number of elements ($\boldsymbol{e}$)	33
SCED brace deformation capacity ($\boldsymbol{\delta_b}$)	169 mm

RS-SCED Brace Mechanism

The mechanism of the RS-SCED brace, shown in schematic form in Figure 2 and illustrated in Figure 3, is different from the mechanisms used by other large-scale SCED braces previously developed [27],[28]. This is because the new RS-SCED brace relies on compression of the ring spring assembly rather than the tension of the prestressing tendon to provide the restoring force and bring the brace back to its original configuration. The brace mechanism consists of 4 main elements: (1) a ring spring assembly that is pre-compressed with one end plate on each of its two ends, (2) a steel prestressing chair that has a steel piston that compresses the ring springs when the brace is under compression, (3) a steel threaded rod that transfers the load from the steel prestressing chair to the ring springs when the brace is under tension, and (4) an outer member that houses the ring springs and transfers the load to the rest of the structure.

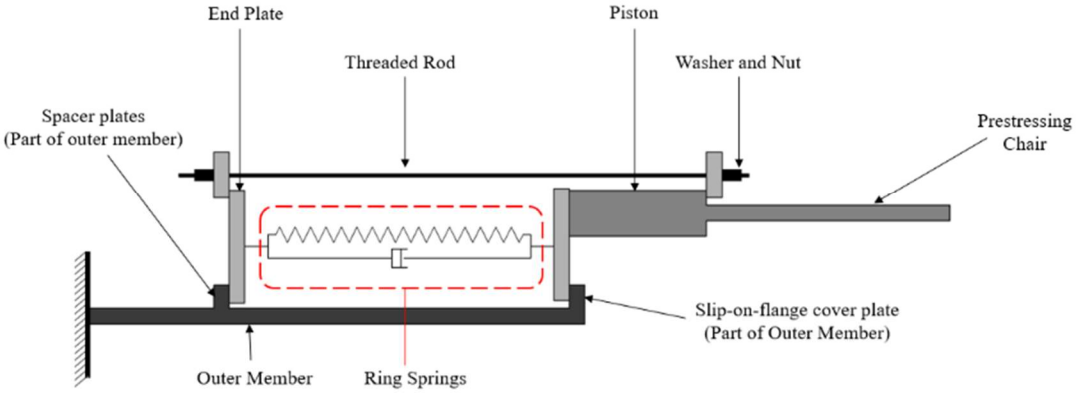

Figure 2: Schematic representation of RS-SCED showing the brace mechanism

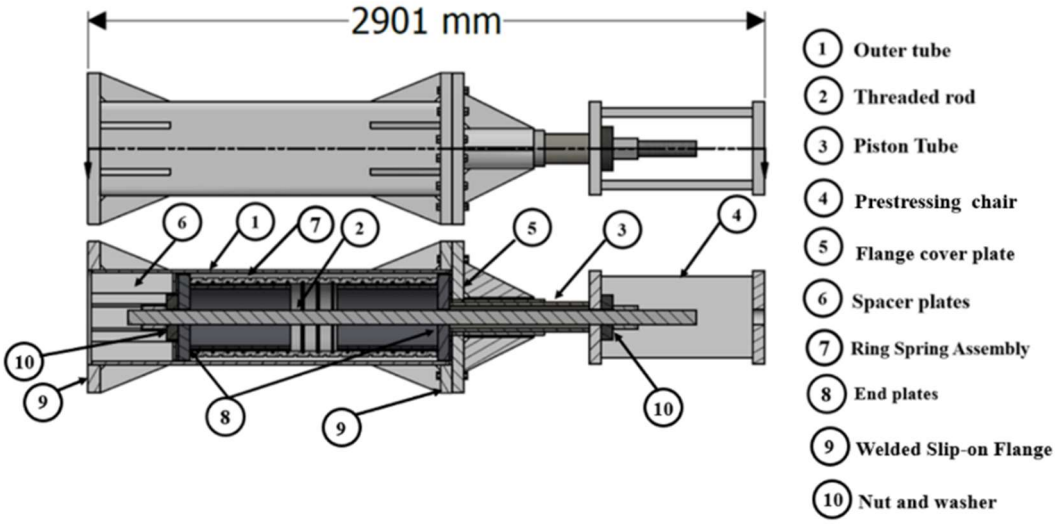

Figure 3: RS-SCED Brace cross-section showing the brace components

Initially, the ring springs are pre-compressed by tensioning the threaded rod during the assembly. Therefore, at its initial state, the piston along with the ring springs are both under compression while the steel threaded rod is under tension. The magnitude of this load is the equivalent to the intended activation load of the SCED brace P_a. Although the spacer plates and the slip-on-flange cover plate are both in contact with the ring assembly, neither of them sustains any significant load at this stage. Therefore, the outer member is not significantly loaded at this initial stage. Similarly, the prestressing chair is not loaded at this stage. Due to the arrangement of the brace components, the ring springs are compressed relative to their initial state regardless of whether the brace is in tension or in compression.

The hysteretic behaviour of the RS-SCED brace is shown in Figure 4. Starting on the tension side, the initial stiffness K_i in the hysteretic response is a result of all the elements deforming together until the tension force overcomes the initial pre-compression of the ring springs P_a, allowing the left end plate to separate from the outer member. After the initial compression force in the springs P_a is exceeded, the SCED brace is 'activated' and the stiffness of the brace is approximately equal to the stiffness of the ring spring loading stiffness K_L. When the brace is in tension, the prestressing chair moves to the right and abuts against the right-side washer plate of the threaded rod. The threaded rod moves to the right pulling the left end plate to the right with it. This results in the ring springs getting compressed between the two end plates, since the right end plate is restrained from moving to the right by means of the slip-on-flange cover plate. The cover plate of the slip-on-flange transfers the load to the outer member which transfers it to the supporting structure of the brace. During this stage of loading, the piston tube as well as the spacer plates are not expected to carry any axial loads. As the brace starts unloading, the ring springs are once again locked in position and do not decompress until the applied tension load decreases below the recoil load of the brace P_R. This is required to overcome the breaking friction force between the interlocked ring springs. During this stage, the stiffness of the brace is once again equal to the initial stiffness K_i. Once the load drops below the recoil load P_R, the brace 'reactivates' and starts decompressing at a stiffness equal to the unloading stiffness of the ring springs K_u. The springs continue to decompress until they reach their initial length.

Like in the tension cycle, the loading stiffness of the brace at the initial stage in compression is equal to the initial stiffness K_i. Once the compressive load exceeds the activation load P_a, the point where the pre-compression in the springs is overcome, the stiffness of the brace at this stage is equal to the loading stiffness of the brace K_L. When the brace is in compression, the piston bears against the right end plate moving it to the left. This results in the ring springs getting compressed between the two end plates since the left end plate is restrained from moving to the left by means of the spaced plates. The spacer plate then transfers the load to outer member which is then transferred to the rest of the structure. During this stage, the threaded rod does not carry any load and thus is free to slide. $F_R K_u K_i$

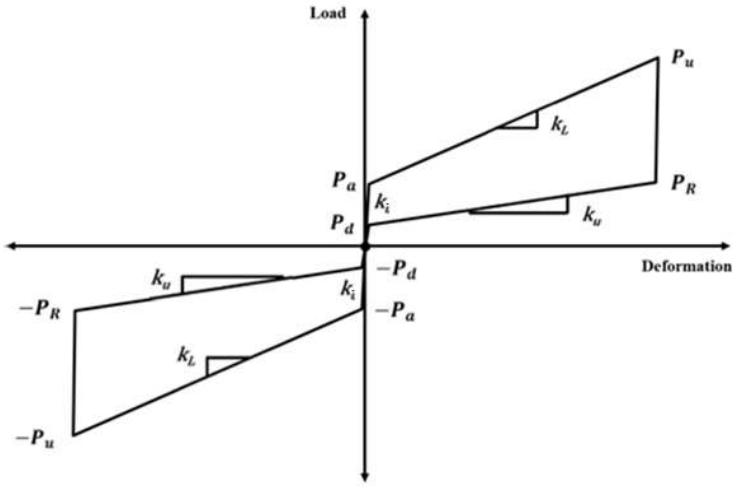

Figure 4: Schematic of the brace after the final step of the hysteresis

CHARACTERIZATION OF RS-SCED BRACE BEHAVIOUR THROUGH EXPERIMENTAL TESTING

The RS-SCED brace is characterized through a test program which includes a frequency dependence test, the ASCE 7-16 Protocol [44], the AISC 341-16 protocol [45] and a capacity test. The test setup is shown in Figure 5 and details of each test are provided in [46].

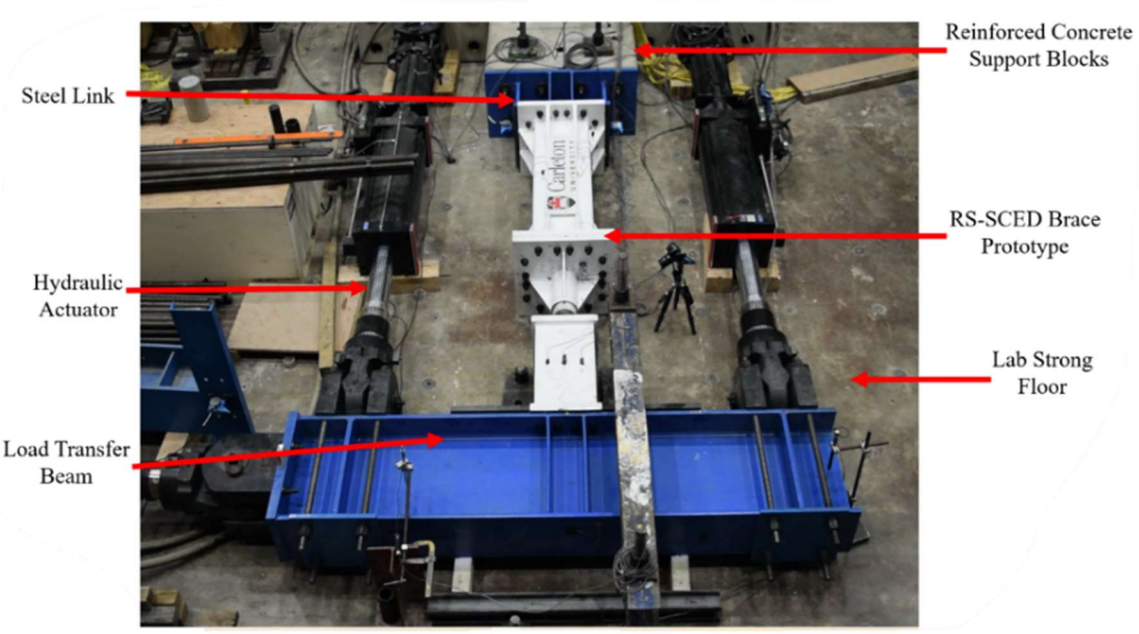

Figure 5:Test setup used for this study at Carleton University structures lab

The frequency dependence test was applied to determine the dynamic performance of the new RS-SCED brace at different loading rates. The RS-SCED is subjected to four fully-reversed sinusoidal cycles of ±10 mm displacement at maximum

displacement rates ranging from 2 mm/s (0.06 Hz) to 45 mm/s (1.43 Hz). The results showed that the hysteretic response, self-centering behavior, post-activation and pre-activation stiffnesses, activation load P_a , recoil load P_R and decompression load P_d, are not significantly affected by the displacement rate.

The prototype test specified in Section 18.6 of ASCE 7-16 [44] is intended to confirm the force-velocity-displacement properties of damping devices and to demonstrate the robustness of individual devices under seismic excitation. The observed hysteresis from this loading protocol was found to be consistent with the theoretical response predicted. The response is stable and repeatable. The pre- and post-activation stiffnesses are consistent for all displacement demands with clearly defined activation force P_a , recoil load P_R and decompression load P_d. The RS-SCED brace response also shows no residual drift with the brace fully capable of maintaining the self-centering behaviour throughout all the cycles in the ASCE 7-16 loading protocol as shown in Figure 6. To check the durability of the RS-SCED brace, the ASCE 7-16 protocol was conducted for a second time upon the completion of the hybrid simulations. Although the pre- and post-activation stiffnesses, as well as the activation force P_a, recoil load P_R and decompression load P_d remain consistent throughout the test, the hysteresis shows a gradual shift in the recoil position of the brace after every cycle. This is caused by the nut on the steel rod becoming a bit loose gradually after repeated cycles. This generated a gap between the nut on the end of the threaded rod and the end plate that is in contact with the spacer plates. In turn, this gap caused a delay between the point at which the brace reaches the neutral position and the end of the threaded rod bearing against the end plate and initiating the tensile cycle. Considering that the number of frequency tests, loading protocols and hybrid tests this brace experienced far exceeds the number of earthquake records that any brace would experience throughout its life cycle, the results demonstrate the durability and robustness of the RS-SCED when subjected to significant loading for a large number of cycles.

The purpose of the AISC 341-16 [45] cyclic testing protocol is to provide evidence that a buckling restrained brace (BRB) satisfies requirements for strength and inelastic deformation. Because the RS-SCED brace is designed to have similar force capacity and applications as a BRB, testing the RS-SCED brace using the AISC 341-16 loading protocol is helpful for assessing its performance. The force-deformation response of the RS-SCED brace, shown in Figure 6, was found to be stable and repeatable at drift levels up to 3%. Like the results shown for the ASCE 7-16 protocol presented in the previous section, the initial and post-activation stiffnesses as well as the activation force P_a, recoil load P_R and decompression load P_d correlate well with the response predicted from the response of the ring spring assembly. There is no observable residual deformation even after being subjected to numerous cycles from both the ASCE and AISC loading protocols. Also, the pre- and post-activation stiffnesses are highly consistent even at high load and deformation demands. The only other noticeable difference between the pre-hybrid test and post hybrid tests was an increase in minor load fluctuation. This is mainly due to the slight increase in friction caused by frequent incidental contact between the bottom of the end plates and the inner surface of the outer tube.

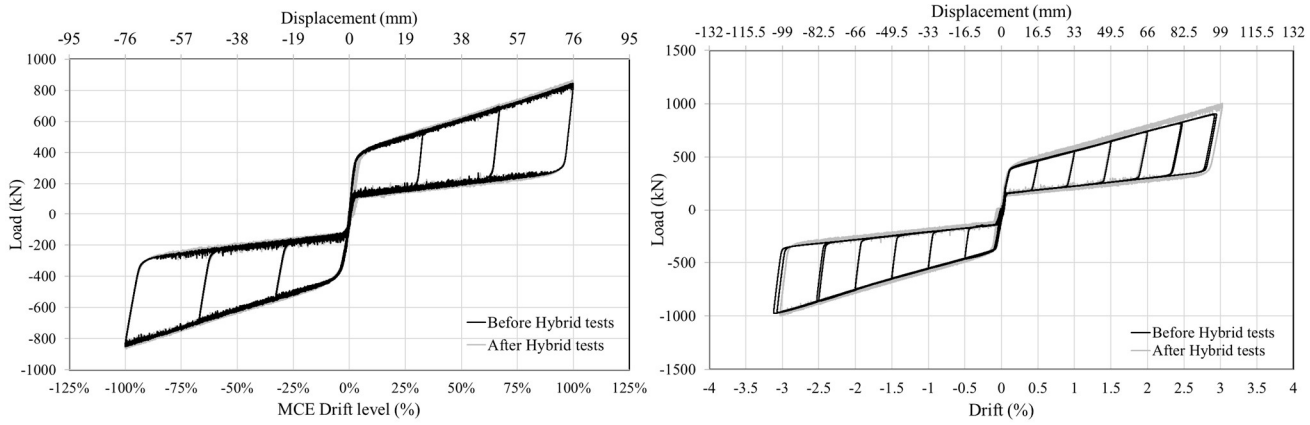

Figure 6: RS-SCED brace response to ASCE 7-16 (left) and AISC 341-16 (right) loading protocol

In this study, the RS-SCED brace is subjected to a loading cycle in which the brace is loaded up to the design drift demand of 4%, which corresponds to 132 mm of axial deformation of the brace. The capacity test is conducted to determine whether the brace can maintain its re-centering capacity at significant inelastic deformation and load demands. It was determined that the RS-SCED is capable of maintaining stable hysteresis with a constant post-activation stiffness at a drift demand of 4% and a maximum load of 1200 kN. The RS-SCED maintains its self-centering behaviour showing no signs of residual deformation up to its maximum design capacity.

HYBRID SIMULATION OF RS-SCED BRACE

Past studies have examined the behaviour of SCED braces under simulated seismic load. The majority of these studies were either quasi-static full-scale tests or shake table tests involving scaled specimens. Quasi static full-scale tests have the limitation

of not being capable of evaluating the effect of the brace response on the global system-level behaviour and performance of the structure. On the other hand, shake table tests are restricted by the test specimen size due to cost of construction and shake table capacity. In this study, a series of hybrid simulations are performed to evaluate the system-level performance of the new RS-SCED brace. The benefits of hybrid simulation include its ability to study the non-linear behaviour of a critical or complex structural component in detail in the laboratory through experimental testing, while at the same time capturing the system-level response of the full-scale structural system in a numerical model. This makes it feasible to determine the realistic behaviour and impact of the physically tested brace on the global response of the structure, without having the need to test the entire structure. To conduct a hybrid simulation, a substructuring approach is followed. In this approach, a structure is separated into experimental and analytical substructures in which the structural mass and damping effects are included in the analytical substructure. A discretized model of the analytical substructure is analyzed by a computer under the effects of static and/or dynamic loading. An earthquake ground acceleration time-history record is used as the input excitation for the model. At each discrete time step, a numerical integration technique is used to solve the equation of motion for the structure and to obtain a target displacement vector at the nodes that couple the analytical substructure with the physical substructure. By means of a middleware controller, static or dynamic hydraulic actuators apply one or more target displacements to the physical substructure and the data-acquisition system comprising of several different measurement sensors and instruments including transducers and load cells record the restoring forces and achieved displacements. The restoring forces are fed back through the middleware to the finite element model of the numerical substructure and into equation of motion of the structure. The equation of motion is then solved again at the next time step. This process is repeated for the duration of the ground motion record.

To determine the effectiveness of the new RS-SCED brace, a model of an 8-storey office building which utilizes RS-SCED braces as the SFRS is developed. The responses of fully numerical models are verified by the results obtained from the hybrid simulation. The building is designed according to the ASCE 7-16 [44] for seismicity of Victoria, BC, Canada, which represents a high seismicity region in Canada where the seismic loads govern the design of the lateral load resisting system. The prototype building is an 8-storey building with plan dimensions of 35 m by 45 m, and an elevation of 32 m. The building has a typical floor height of 4 m and column spacing of 7 m in the north south (N-S) direction and 9 m in the east-west direction (E-W). The ring spring SCED brace is implemented in a chevron brace configuration. In this configuration, two RS-SCED braces are placed horizontally acting in parallel under lateral loading. Placing the braces horizontally allows the ratio between the brace deformation and floor deformation to be equal to 1, which is higher than the ratio for a traditional diagonal brace configuration. This is beneficial as it enables the full utilization of the brace deformation capacity in resisting floor drift. Another advantage of using a chevron brace configuration is the ability to use two braces in parallel in a single frame which doubles the lateral load capacity of the frame. Additional information regarding the prototype buildings and models are provided in [46]. An elevation view of the prototype building and an illustration of the analytical model used for the hybrid simulation are shown in Figure 7.

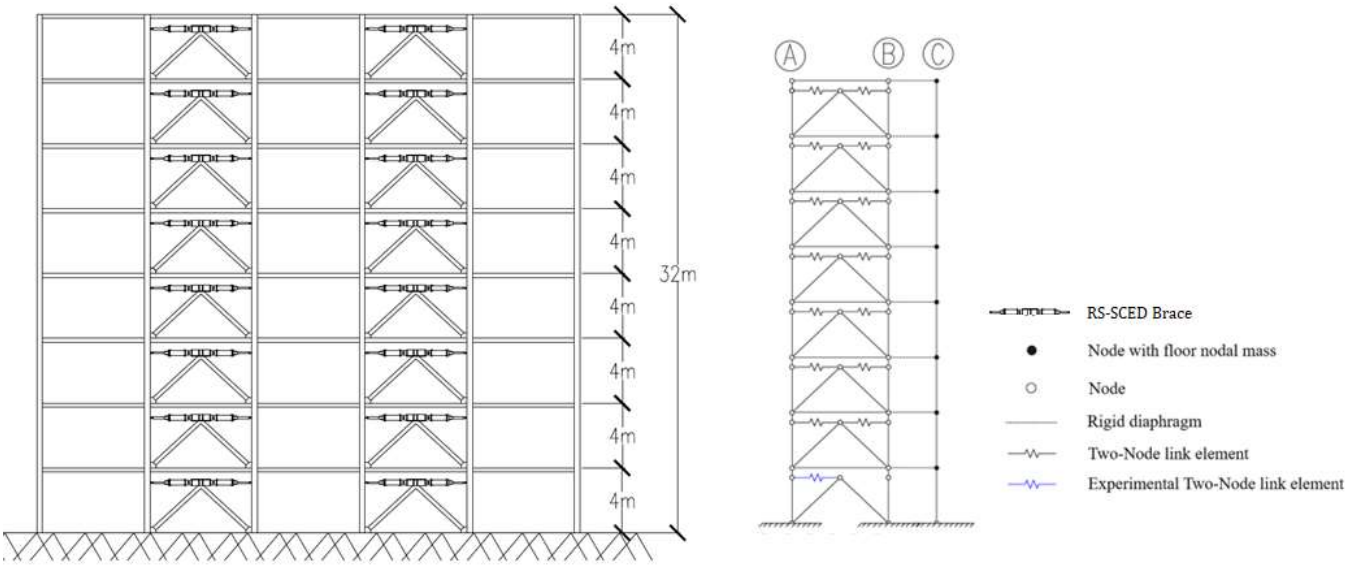

Figure 7: Building elevation of prototype building and analytical model used for the hybrid simulation

To meet the goal of the hybrid simulation of assessing the system level behaviour of the structure under different seismic hazards, the structures are subjected to four different historical earthquake ground motions. These earthquake ground motions are chosen to cover a wide range of frequencies as expressed by the ratio (PHA/PHV) between peak horizontal acceleration (in g) to the peak horizontal velocity (in m/s) as shown in Table 2. Among the four earthquake records, one of the records is a near-

field record while the other three earthquake records are far-field records. The earthquake records are scaled so that the spectral acceleration at the first period of vibration of the structure (T_1 = 1.2 s) matches or exceeds the response spectrum of the structure at that period for Victoria, BC at the Frequently Occurring Earthquake (FOE), Design Based Earthquake (DBE) and Maximum Credible Earthquake (MCE) hazard levels. These seismic hazards correspond to a 50%, 10% and 2% probability of exceedance in 50-years, respectively. However, the Chi-Chi record is only scaled to MCE and DBE hazard levels.

Table 2: Unscaled earthquake record data and scaling intensity used for the hybrid simulation study

Earthquake Record	PGA (g)	PGV (m/s)	PGA/PGV (g*s/m)	NF or FF
Northridge: Canyon Country-WLC	0.48	0.45	1.067	FF
Kobe: Shin-Osaka	0.24	0.38	0.632	FF
Loma Prieta: Capitola	0.53	0.35	1.514	FF
ChiChi: TCU 067	0.29	0.29	0.272	NF

Comparison of Hybrid Simulation and Fully Analytical Model

To evaluate the effectiveness of the numerical model in predicting the non-linear seismic response of a multi-storey building utilizing RS-SCED braces as the SFRS, the full-scale hybrid test results are compared with the results from a fully-analytical finite element model. To compare the result of both systems, four different response parameters were evaluated at different hazard levels and summarized in Table 3 to Table 5. The four response parameters chosen are the maximum first floor drift Δ_1/h_s, the maximum first floor residual drift Δ_{r1}/h_s, the maximum floor acceleration of the first floor a_{f1}, and the maximum roof drift Δ_{roof}/h_{total}. The results show a good correlation between the analytical and the hybrid simulation results for all 4 parameters considered at each hazard level. Under FOE and DBE hazard level earthquakes the maximum inter-storey drift at the first-floor level is low and the maximum residual drift level did not exceed 0.1% for any of the records, maintaining the structure's self-centering ability. The structures experience a relatively large first floor acceleration a_f as a result of the high initial stiffness of the RS-SCED braces. At the MCE hazard level, the maximum inter-storey drift is comparable to the design drift limit, which indicates that the design method achieved the intended outcome. This is to be expected due to the higher seismic demand on the structure at this hazard level. The residual drift of the structure at this higher seismic hazard level is the highest among all three hazard levels but still the highest residual drift at the first-floor level is only 0.11%. This indicates that the RS-SCED braces can maintain the self-centering capability even at this higher hazard level.

Table 3: Summary of results under FOE hazard level

	Northridge		Kobe		Loma Prieta	
	Hybrid	**Model**	**Hybrid**	**Model**	**Hybrid**	**Model**
$\boldsymbol{\Delta_1/h_s}$	0.40%	0.38%	0.17%	0.18%	0.25%	0.22%
$\boldsymbol{\Delta_{r1}/h_s}$	0.02%	0.03%	0.06%	0.00%	0.05%	0.01%
$\boldsymbol{a_{f1}}$	0.52	0.51	0.40	0.41	0.53	0.68
$\boldsymbol{\Delta_{roof}/h_{total}}$	0.34%	0.32%	0.45%	0.42%	0.31%	0.31%

Table 4: Summary of results under DBE hazard level

	Northridge		Kobe		Loma Prieta		Chi-Chi	
	Hybrid	**Model**	**Hybrid**	**Model**	**Hybrid**	**Model**	**Hybrid**	**Model**
$\boldsymbol{\Delta_1/h_s}$	1.09%	1.18%	0.81%	0.74%	0.57%	0.56%	0.51%	0.52%
$\boldsymbol{\Delta_{r1}/h_s}$	0.06%	0.05%	0.09%	0.02%	0.08%	0.02%	0.01%	0.00%
$\boldsymbol{a_{f1}}$	0.74	0.93	0.70	0.70	0.72	0.86	0.37	0.49
$\boldsymbol{\Delta_{roof}/h_{total}}$	0.79%	0.82%	0.51%	0.52%	0.44%	0.50%	0.69%	0.67%

Table 5: Summary of results under MCE hazard level

	Northridge		Kobe		Loma Prieta		Chi-Chi	
	Hybrid	**Model**	**Hybrid**	**Model**	**Hybrid**	**Model**	**Hybrid**	**Model**
$\boldsymbol{\Delta_1/h_s}$	2.40%	2.34%	1.22%	1.17%	1.16%	1.23%	2.34%	2.45%
$\boldsymbol{\Delta_{r1}/h_s}$	0.11%	0.09%	0.02%	0.02%	0.06%	0.01%	0.00%	0.01%
$\boldsymbol{a_{f1}}$	1.10	1.13	1.10	1.10	0.93	1.02	0.60	0.71
$\boldsymbol{\Delta_{roof}/h_{total}}$	1.76%	1.86%	0.71%	0.71%	0.91%	0.91%	1.34%	1.39%

Figure 8 shows the hysteretic response of the RS-SCED braces in the first floor. The results show that the analytical model accurately predicts the pre- and post-activation response of the braces while capturing the full flag shape hysteresis of the brace. The activation force, post-activation stiffness, recoil load and decompression load measured in all 11 hybrid tests matched their

design values. The major difference between the hybrid simulation and analytical model hysteresis response is the stiffness transitions that occur each time the ring springs compress or decompress. The actual hysteresis of the RS-SCED braces, measured during the hybrid tests, show that the transition between: a) the initial stiffness to loading stiffness during activation, b) initial stiffness to unloading stiffness at the onset of decompression, and c) from the unloading stiffness back to the initial stiffness at the decompression load level unloading stiffness and initial stiffness during the decompression of the springs, are not sharp corners as assumed in the constitutive material model. This is because the ring springs within the assembly do not lock or unlock all at once but rather progressively start moving relative to each other resulting in a more gradual stiffness transition. The sharp stiffness transition, used to model the flag shaped hysteretic behaviour of the brace, has been shown to typically result in the upper bound estimates of the acceleration, often resulting in overestimation of the system acceleration [48]. The stiffness transition that has the greatest effect on this overestimation is the transition from the unloading stiffness back to the initial stiffness of the brace which occurs when the applied load decreases to the decompression load. Although the acceleration response was often accurately predicted as shown in Table 3 to Table 5, certain models showed the acceleration was overestimated. This occurred when the structure was subjected to the Loma Prieta and the Chi-Chi earthquake records. The overestimation is attributed to the sharp stiffness transitions observed in the analytical hysteretic response.

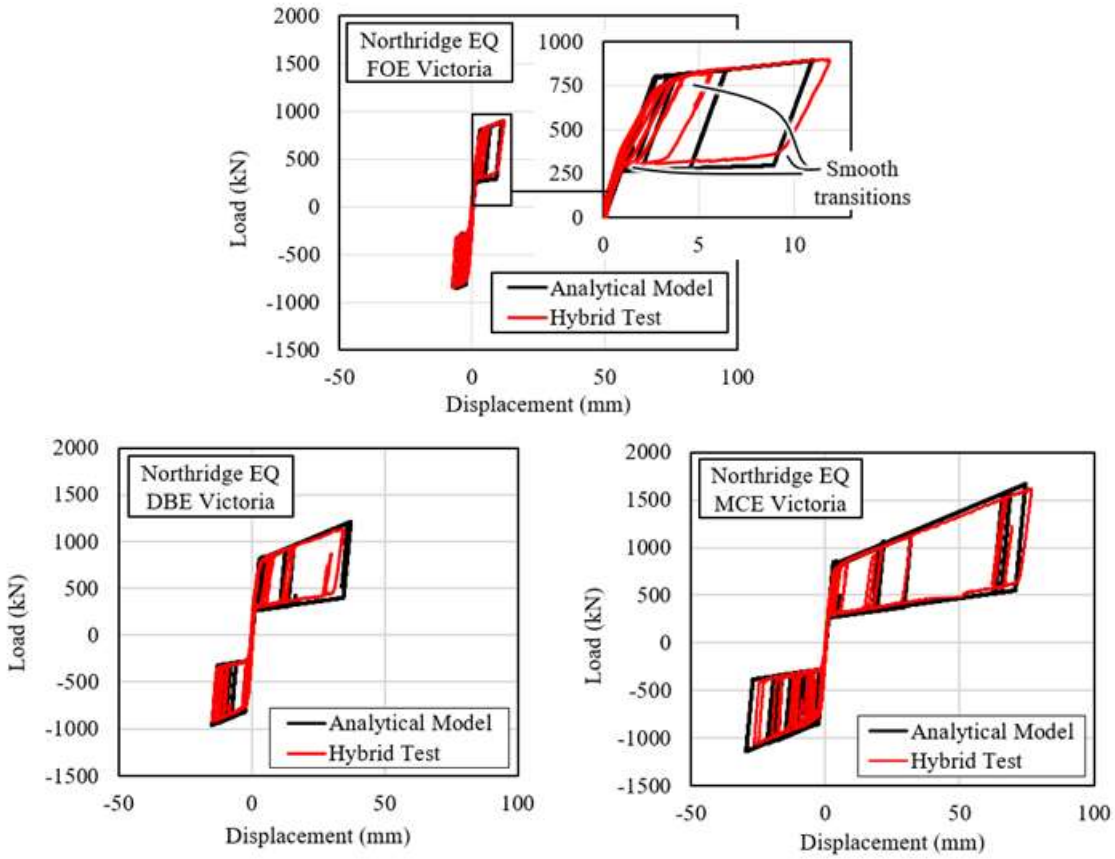

Figure 8: Comparison of force-deformation hysteretic response for the Northridge earthquake

Figure 9 shows the time history response of the first floor RS-SCED brace deformation and roof drift for the Northridge earthquake at the MCE hazard level. Similar to the hysteretic response, the brace deformation time history response predicted by the analytical model also correlated very well with the brace deformation time history response measured during the hybrid simulation, including at the peak of the responses. Despite having minor discrepancy in the prediction of some of the post peak responses, the analytical model accurately predicted the peak deformation of each response. Overall, the comparison of the analytical model and hybrid simulation results validates the use of the analytical modelling technique proposed.

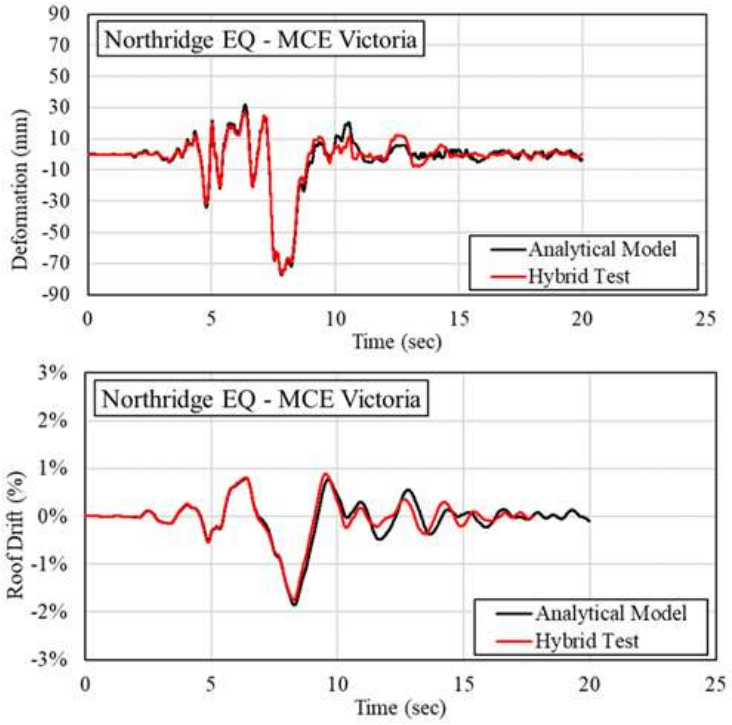

Figure 9: Brace deformation and roof-drift time-history for the Northridge earthquake record at MCE hazard level

CONCLUSIONS

The motivation to overcome the shortcoming of large permanent deformation after exposure to major earthquake in BRBF, ductile MRF and other SFRS systems has led to the development of self-centering systems including rocking walls and self-centering MRFs. However, the use of self-centering braces is a more appropriate option for rehabilitation of structures as it is less disruptive than installation of rocking wall or self-centering MRFs. Previously developed Self-Centering Energy Dissipative (SCED) braces had limited load capacity or were required to be very long to accommodate for large displacements, limiting their applicability in real structures. This study aimed to develop a new high-capacity SCED brace with a more compact design using ring springs, hence, the brace was named the Ring Spring Self-Centering Energy Dissipative Brace (RS-SCED).

The first phase of this study focused on the development and design of a full-scale brace with a capacity that is comparable to a BRB and that could be used in a multi-storey office building. Accordingly, an RS-SCED brace was designed and built with a length of 3 m, a capacity of 1400 kN, and a deformation capacity of 165 mm. The brace was compact enough so that two such braces can be added to a single bay frame in a chevron bracing configuration. The RS-SCED brace was constructed and tested according to the ASCE 7-16 and the AISC 341-16 protocols for testing seismic dampers and buckling restrained braces, respectively. The results showed a repeatable, consistent, and predictable response that correlated with the theoretical force-deformation hysteretic response very well. The response of the brace remained consistent even after repeated testing and many loading cycles. The brace was also loaded cyclically at different frequencies to determine if its behaviour was rate dependent, and the results showed that the brace exhibits consistent pre- and post-activation stiffness and force over a wide range of load frequencies. During the tests, the brace was loaded up to a load and deformation of 1200 kN and 132 mm, respectively.

The second phase of this study investigated the system-level response of an 8-storey office building with RS-SCED braces. To accurately capture the nonlinear response of the proposed RS-SCED brace and its influence on the global system-level response of the prototype structures, 11 hybrid simulations were conducted. The structures were subjected to 4 different earthquake records which represented a wide range of frequency contents including one near-field and 3 far-field earthquake records. The hybrid simulation results were compared with purely numerical models. To model the analytical structures, a new constitutive material was created in OpenSees to accurately represent the force-deformation response of the RS-SCED brace. Comparison of the system level response between the hybrid simulation and the numerical analysis showed very good correlation.

ACKNOWLEDGMENTS

The authors would like to acknowledge RingFeder Power Transmission, and in particular Edward Cole and Lars Jahnel for their technical support and providing the material for the project. The authors would also like to acknowledge CFI support for the hybrid simulation test facilities, NSERC for support of the project with funding through the Discovery Grants program.

REFERENCES

[1] C. Comartin, M. Greene, and S. Tubbesing, *The Hyogo-ken Nanbu earthquake: Great Hanshin Earthquake Disaster, January 17, 1995: preliminary reconnaissance report*. Oakland, California, 1995.

[2] R. Eguchi, "Direct economic losses in the Northridge earthquake: a three-year post-event perspective," *Earthq. Spectra*, vol. 14, no. 2, pp. 245–264, 1998.

[3] K. Kaga, "Vestibular sensitivity and sense of inclination," *J. Cogn. Sci. (Seoul).*, vol. 7, no. 1, pp. 16–22, 2005.

[4] M. Seto, "Sensitivity and memory of body inclination (part 1) – Ability to restore to vertical position," *Quilibrium Res.*, vol. 55, no. 5, p. 204, 1996.

[5] M. Fujii, "Damage to an repair of foundations of residential buildings in liquefied areas inHygoken-Nanbu earthquake.," *Soil Found.*, vol. 46, pp. 9–12, 2002.

[6] Y. Iwata, K. Sugimioto, and H. Kuwamura, "Reparability limit of steel structural buildings: Study on performance-based design of steel structural buildings Part 2," *J. Struct. Constr. Eng.*, vol. 588, pp. 165–172, 2005.

[7] C. M. Ramirez and E. Miranda, "Significance of residual drifts in building earthquake loss estimation," *Earthq. Eng. Struct. Dyn.*, vol. 41, no. 11, pp. 1477–1493, 2012, doi: 10.1002/eqe.2217.

[8] M. Kato, "Seismic performance and damage evaluation of drywall partitions," *J. Struct. Constr. Eng.*, vol. 614, pp. 139–146, 2007.

[9] J. McCormick, Y. Matsuoka, P. Pan, and M. Nakashima, "Evaluation of Non-Structural Partition Walls and suspended ceiling systems through a shake table study," in *Proc. of the 2008 ASCE Structures Congress.*, 2008.

[10] J. Erochko, C. Christopoulos, R. Tremblay, and H. Choi, "Residual Drift Response of SMRFs and BRB Frames in Steel Buildings Designed according to ASCE 7-05," *J. Struct. Eng.*, vol. 137, no. 5, pp. 589–599, 2010, doi: 10.1061/(asce)st.1943-541x.0000296.

[11] C. Fang, Q. Zhong, W. Wang, S. Hu, and C. Qiu, "Peak and residual responses of steel moment-resisting and braced frames under pulse-like near-fault earthquakes," *Eng. Struct.*, vol. 177, no. October, pp. 579–597, 2018, doi: 10.1016/j.engstruct.2018.10.013.

[12] ASCE- American Society of Civil Engineers, *Minimum Design Loads for Buildings and Other Structures*, ASCE/SEI 7. Reston, VA: American Society of Civil Engineers, 2005

[13] J. J. Ajrab, G. Pekcan, and J. B. Mander, "Rocking Wall–Frame Structures with Supplemental Tendon Systems," *J. Struct. Eng.*, vol. 130, no. 6, pp. 895–903, Jun. 2004, doi: 10.1061/(ASCE)0733-9445(2004)130:6(895).

[14] L. Panian, M. Steyer, and S. Tipping, "An innovative approach to earthquake safety and concrete construction," *J. Post Tens. Inst.*, vol. 5, no. 1, pp. 7–16, 2007.

[15] A. Wada, Z. Qu, H. Ito, S. Motoyui, H. Sakata, and K. Kasai, "Seismic retrofit using rocking walls and steel dampers," in *ATC/SEI Conf. on Improving the Seismic Performance of Existing Buildings and Other Structures*, 2009.

[16] G. G. Deierlein, X. Ma, M. Eatherton, J. Hajjar, H. Krawinkler, and T. Takeuchi, "Collaborative research on development of innovative steel braced frame systems with controlled rocking and replaceable fuses," in *Proc., 6th Int. Conf. on Urban Earthquake Engineering*, 2009, pp. 413–416.

[17] Z. Qu, A. Wada, S. Motoyui, H. Sakata, and S. Kishiki, "Pin-supported walls for enhancing the seismic performance of building structures," *Earthq. Eng. Struct. Dyn.*, vol. 41, no. 14, pp. 2075–2091, Nov. 2012, doi: 10.1002/eqe.2175.

[18] B. Janhunen, S. Tipping, J. Wolfe, and D. Mar, "Seismic retrofit of a 1960s steel moment- frame high-rise using a pivoting spine," in *Proc. 2012 Annual Meeting of the Los Angeles Tall Buildings Structural Design Council*, 2012.

[19] M. M. Garlock, R. Sause, and J. M. Ricles, "Behavior and Design of Posttensioned Steel Frame Systems," *J. Struct. Eng.*, vol. 133, no. 3, pp. 389–399, Mar. 2007, doi: 10.1061/(ASCE)0733-9445(2007)133:3(389).

[20] A. I. Dimopoulos, T. L. Karavasilis, G. Vasdravellis, and B. Uy, "Seismic design, modelling and assessment of self-centering steel frames using post-tensioned connections with web hourglass shape pins," *Bull. Earthq. Eng.*, vol. 11, no. 5, pp. 1797–1816, Oct. 2013, doi: 10.1007/s10518-013-9437-4.

[21] A. S. Tzimas, A. I. Dimopoulos, and T. L. Karavasilis, "EC8-based seismic design and assessment of self-centering post-tensioned steel frames with viscous dampers," *J. Constr. Steel Res.*, vol. 105, pp. 60–73, Feb. 2015, doi: 10.1016/j.jcsr.2014.10.022.

[22] A. I. Dimopoulos, A. S. Tzimas, T. L. Karavasilis, and D. Vamvatsikos, "Probabilistic economic seismic loss estimation in steel buildings using post-tensioned moment-resisting frames and viscous dampers," *Earthq. Eng. Struct. Dyn.*, vol. 45, no. 11, pp. 1725–1741, Sep. 2016, doi: 10.1002/eqe.2722.

[23] A. S. Tzimas, G. S. Kamaris, T. L. Karavasilis, and C. Galasso, "Collapse risk and residual drift performance of steel buildings using post-tensioned MRFs and viscous dampers in near-fault regions," *Bull. Earthq. Eng.*, vol. 14, no. 6, pp. 1643–1662, Jun. 2016, doi: 10.1007/s10518-016-9898-3.

[24] F. Freddi, C. A. Dimopoulos, and T. L. Karavasilis, "Rocking damage-free steel column base with friction devices: design procedure and numerical evaluation," *Earthq. Eng. Struct. Dyn.*, vol. 46, no. 14, pp. 2281–2300, Nov. 2017, doi: 10.1002/eqe.2904.

[25] J. A. . Erochko, "Improvements to the Design and Use of Post-Tensioned by Jeffrey A . Erochko A thesis submitted in conformity with the requirements for the degree of Doctor of Philosophy , Graduate Department of Civil Engineering , University of Toronto © Copyright by Jef," 2013.
[26] National Resources Canada, *Survey of commercial and institutional energy use: Buildings 2009*. Ottawa, 2013.
[27] C. Christopoulos, R. Tremblay, H.-J. Kim, and M. Lacerte, "Self-Centering Energy Dissipative Bracing System for the Seismic Resistance of Structures: Development and Validation," *J. Struct. Eng.*, vol. 134, no. 1, pp. 96–107, Jan. 2008, doi: 10.1061/(ASCE)0733-9445(2008)134:1(96).
[28] J. Erochko, C. Christopoulos, and R. Tremblay, "Design, Testing, and Detailed Component Modeling of a High-Capacity Self-Centering Energy-Dissipative Brace," *J. Struct. Eng.*, vol. 141, no. 8, p. 04014193, 2014, doi: 10.1061/(asce)st.1943-541x.0001166.
[29] J. Erochko, C. Christopoulos, and R. Tremblay, "Design and Testing of an Enhanced-Elongation Telescoping Self-Centering Energy-Dissipative Brace," *J. Struct. Eng.*, vol. 141, no. 6, p. 04014163, Jun. 2015, doi: 10.1061/(ASCE)ST.1943-541X.0001109.
[30] Z. Zhou, Q. Xie, X. C. Lei, X. T. He, and S. P. Meng, "Experimental Investigation of the Hysteretic Performance of Dual-Tube Self-Centering Buckling-Restrained Braces with Composite Tendons," *J. Compos. Constr.*, vol. 19, no. 6, p. 04015011, 2015, doi: 10.1061/(asce)cc.1943-5614.0000565.
[31] H. Wang, X. Nie, and P. Pan, "Development of a self-centering buckling restrained brace using cross-anchored pre-stressed steel strands," *J. Constr. Steel Res.*, vol. 138, pp. 621–632, 2017, doi: 10.1016/j.jcsr.2017.07.017.
[32] L. Xu, X. Fan, and Z. Li, "Experimental behavior and analysis of self-centering steel brace with pre-pressed disc springs," *J. Constr. Steel Res.*, vol. 139, pp. 363–373, 2017, doi: 10.1016/j.jcsr.2017.09.021.
[33] L. H. Xu, X. S. Xie, and Z. X. Li, "A self-centering brace with superior energy dissipation capability: Development and experimental study," *Smart Mater. Struct.*, vol. 27, no. 9, p. 95017, 2018, doi: 10.1088/1361-665X/aad5b0.
[34] L.-H. Xu, X.-S. Xie, S.-Q. Yao, and Z.-X. Li, "Hysteretic behavior and failure mechanism of an assembled self-centering brace," *Bull. Earthq. Eng.*, no. 0123456789, 2019, doi: 10.1007/s10518-019-00590-8.
[35] A. Filiatrault, R. Tremblay, and R. Kar, "Performance Evaluation of Friction Spring Seismic Damper," *J. Struct. Eng.*, vol. 126, no. 4, pp. 491–499, Apr. 2000, doi: 10.1061/(ASCE)0733-9445(2000)126:4(491).
[36] A. S. Issa and M. S. Alam, "Experimental and numerical study on the seismic performance of a self-centering bracing system using closed-loop dynamic (CLD) testing," *Eng. Struct.*, vol. 195, no. August 2018, pp. 144–158, 2019, doi: 10.1016/j.engstruct.2019.05.103.
[37] N. Bishay-Girges, "Sesimic protection of atructures using passive control system," p. 271, 2004.
[38] H. H. Khoo, C. Clifton, J. Butterworth, G. MacRae, S. Gledhill, and G. Sidwell, "Development of the self-centering Sliding Hinge Joint with friction ring springs," *J. Constr. Steel Res.*, vol. 78, pp. 201–211, 2012, doi: 10.1016/j.jcsr.2012.07.006.
[39] H. H. Khoo, C. Clifton, J. Butterworth, and G. Macrae, "Experimental study of full-scale self-centering sliding hinge joint connections with friction ring springs," *J. Earthq. Eng.*, vol. 17, no. 7, pp. 972–977, 2013, doi: 10.1080/13632469.2013.787378.
[40] S. Gary, G. Djojo, C. Clifton, and R. S. Henry, "Experimental validation of Rocking CBFs with Double Acting Ring Springs," pp. 1–8, 2017.
[41] W. Wang, C. Fang, Y. Zhao, R. Sause, S. Hu, and J. Ricles, "Self-centering friction spring dampers for seismic resilience," *Earthq Eng Struct Dyn.* vol. 48 no. 9, pp. 1045-1065, 2019. doi: 10.1002/eqe.3174
[42] A.S. Issa and M.S. Alam, "Seismic performance of a novel single and double spring-based piston bracing," *J Struct Eng*. vol. 145, no. 2:04018261, 2019, doi: 10.1061/(ASCE)ST.1943-541X.0002245.
[43] RingFeder, "RingFeder: Friction Springs," Westwood, NJ, 2004.
[44] ASCE- American Society of Civil Engineers, *Minimum Design Loads and Associated Criteria for Buildings and Other Structures*, ASCE/SEI 7. Reston, VA: American Society of Civil Engineers, 2017.
[45] AISC, "Seismic Provisions for Structural Steel Buildings," *Seism. Provisions Struct. Steel Build.*, p. 402, 2016.
[46] A. Hassan, "Development and Testing of New Ring Spring Self-Centering Energy Dissipative (RS-SCED) Braces for Seismic Resilience of Buildings and Bridges," [Doctoral thesis, Carleton Univeristy], Carleton University Research Virtual Environment, 2020, doi: https://doi.org/10.22215/etd/2020-14959.
[47] NRCC (National Research Council of Canada), National Building Code of Canada, 2015 ed. Ottawa, 2015.
[48] L. Wiebe and C. Christopoulos, "Characterizing acceleration spikes due to stiffness changes in nonlinear systems," Earthq. Eng. Struct. Dyn., vol. 39, no. 14, pp. 1653–1670, Nov. 2010, doi: 10.1002/eqe.1009.
[49] ATC, "Quantification of building seismic performance factors," *FEMA P695*, 2009.